Cross-field Propagation of Plasma Irregularities:Numerical Results Relevant for Macagnetopause Investigation

Marius M. Echim [a]   Joseph Lemaire [b]

[a] Institute for Space Sciences, Bucharest, Romania
[b]Institut d'Aéronomie Spatiale de Belgique, Bruxelles

Mechanisms/models for plasma transfer

Mechanisms/models for plasma transfer

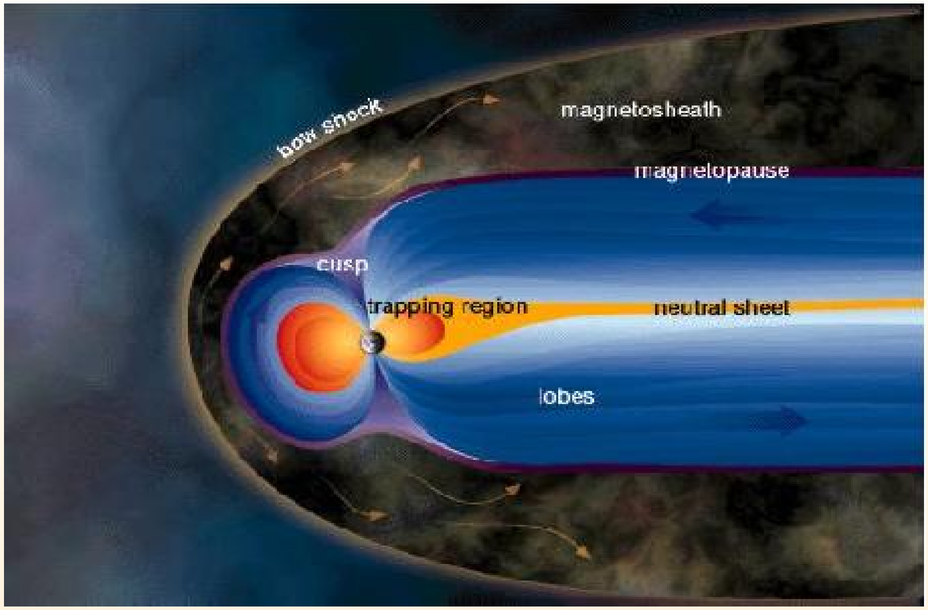

- magnetic reconnection: steady-state, large scale (Dungey, 1961; Petchek, 1964; Vasyliunas, 1976; Sonnerup, 1981), time-dependent (Pudovkin and Semenov, 1985, Kiendl et al., 1992), ...

Mechanisms/models for plasma transfer

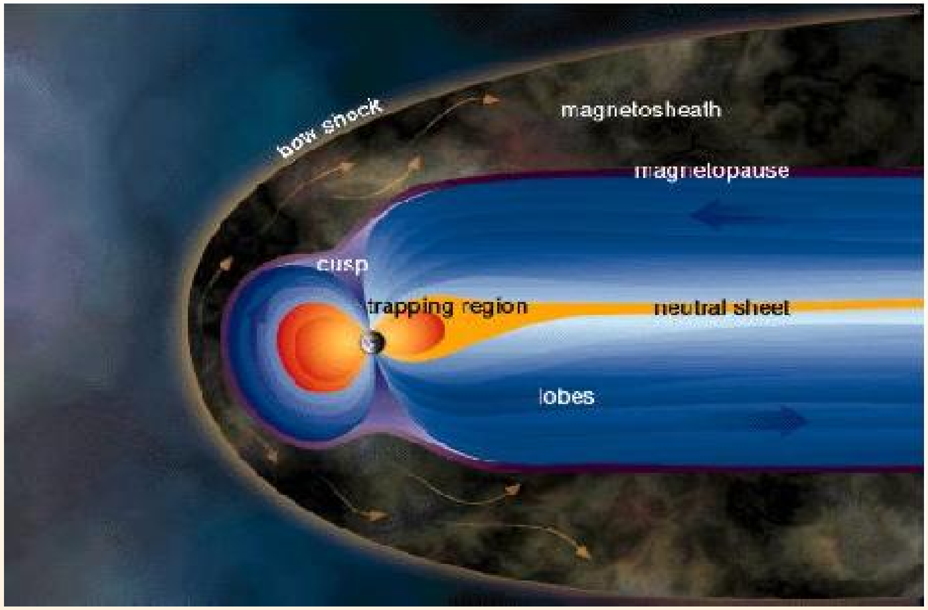

- magnetic reconnection: steady-state, large scale (Dungey, 1961; Petchek, 1964; Vasyliunas, 1976; Sonnerup, 1981), time-dependent (Pudovkin and Semenov, 1985, Kiendl et al., 1992), ...
- Kelvin-Helmholtz instability at the magnetopause (Dungey, 1955; Southwood, 1968; Fujimoto and Terasawa, 1991)

Mechanisms/models for plasma transfer

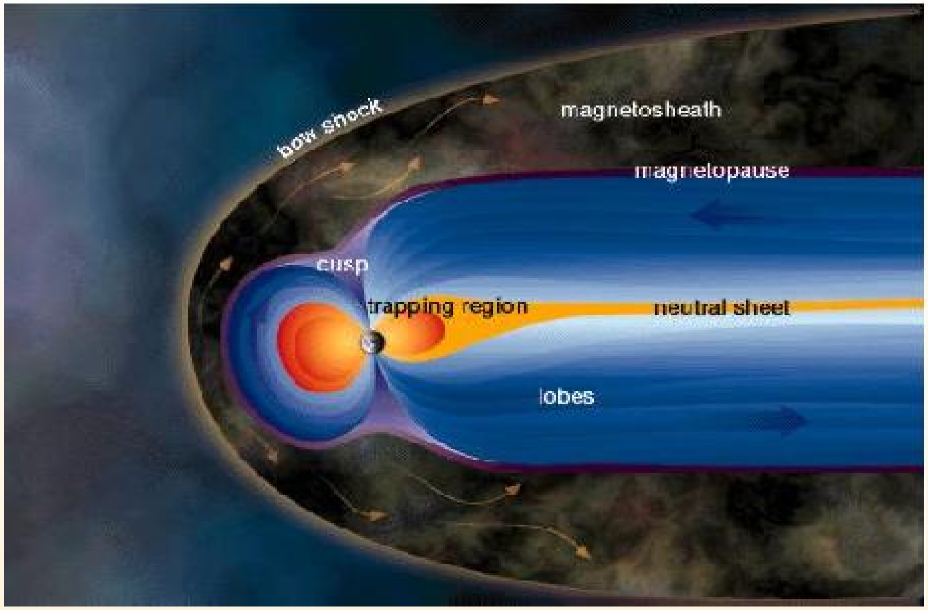

- magnetic reconnection: steady-state, large scale (Dungey, 1961; Petchek, 1964; Vasyliunas, 1976; Sonnerup, 1981), time-dependent (Pudovkin and Semenov, 1985, Kiendl et al., 1992), ...
- Kelvin-Helmholtz instability at the magnetopause (Dungey, 1955; Southwood, 1968; Fujimoto and Terasawa, 1991)
- diffusion(Tsurutani and Thorne, 1982; Winske and Omidi, 1995)

Mechanisms/models for plasma transfer

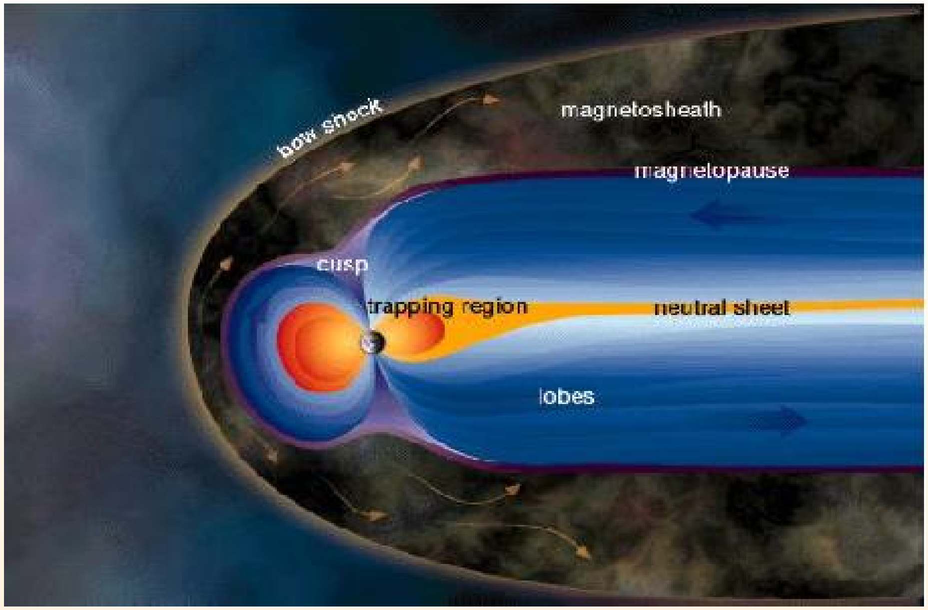

- magnetic reconnection: steady-state, large scale (Dungey, 1961; Petchek, 1964; Vasyliunas, 1976; Sonnerup, 1981), time-dependent (Pudovkin and Semenov, 1985, Kiendl et al., 1992), ...
- Kelvin-Helmholtz instability at the magnetopause (Dungey, 1955; Southwood, 1968; Fujimoto and Terasawa, 1991)
- diffusion(Tsurutani and Thorne, 1982; Winske and Omidi, 1995)
- pressure pulses (Sibeck et al., 1989, 1990; Lin et al., 1996)

Mechanisms/models for plasma transfer

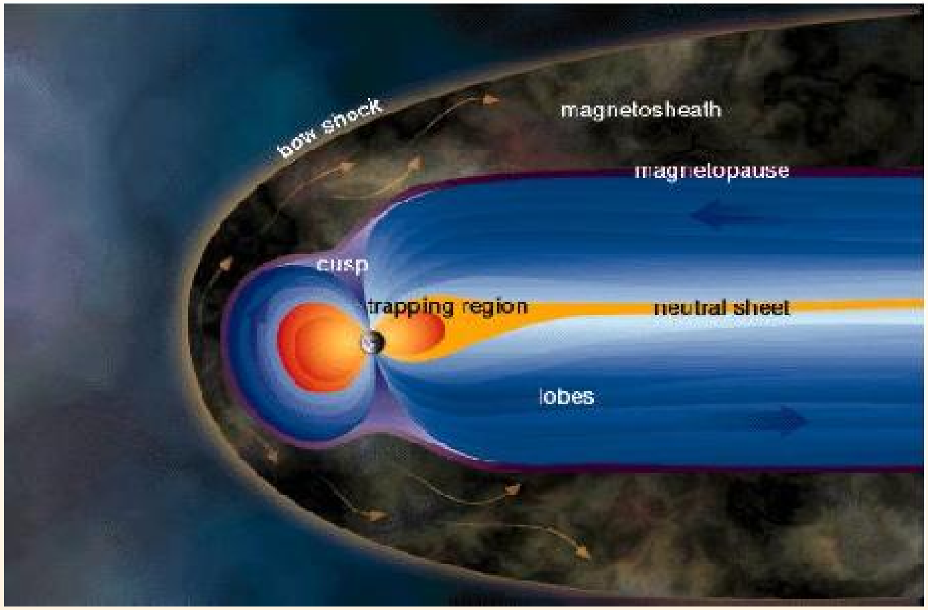

- magnetic reconnection: steady-state, large scale (Dungey, 1961; Petchek, 1964; Vasyliunas, 1976; Sonnerup, 1981), time-dependent (Pudovkin and Semenov, 1985, Kiendl et al., 1992), ...
- Kelvin-Helmholtz instability at the magnetopause (Dungey, 1955; Southwood, 1968; Fujimoto and Terasawa, 1991)
- diffusion(Tsurutani and Thorne, 1982; Winske and Omidi, 1995)
- pressure pulses (Sibeck et al., 1989, 1990; Lin et al., 1996)
- impulsive penetration (Lemaire, 1976, 1985; Heikkila, 1982; Woch and Lundin, 1992)

Collective dynamics of plasma irregularities

- plasmoids: laboratory (Bostick, 1956), active experiments in space (Haerendel, 1976), large active space structures (Hastings and Gatsonis, 1989), magnetotail (Hones, 1982), solar ejecta (Burlaga, 1982), magnetosheath (Lemaire and Roth, 1981)

Collective dynamics of plasma irregularities

- plasmoids: laboratory (Bostick, 1956), active experiments in space (Haerendel, 1976), large active space structures (Hastings and Gatsonis, 1989), magnetotail (Hones, 1982), solar ejecta (Burlaga, 1982), magnetosheath (Lemaire and Roth, 1981)

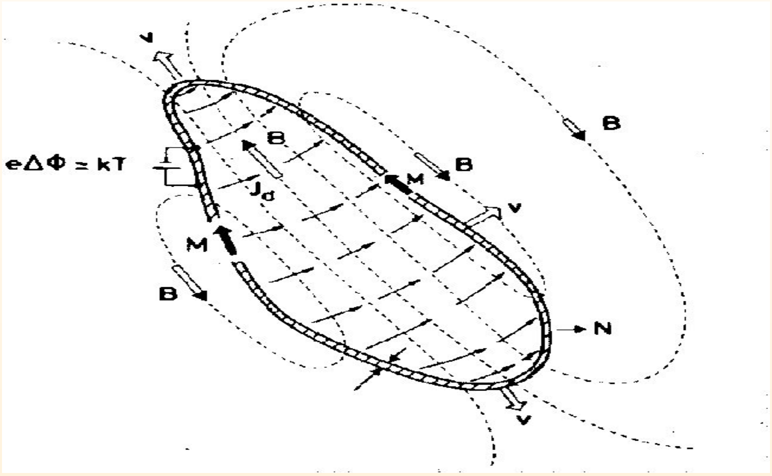

Collective dynamics of plasma irregularities

- plasmoids: laboratory (Bostick, 1956), active experiments in space (Haerendel, 1976), large active space structures (Hastings and Gatsonis, 1989), magnetotail (Hones, 1982), solar ejecta (Burlaga, 1982), magnetosheath (Lemaire and Roth, 1981)

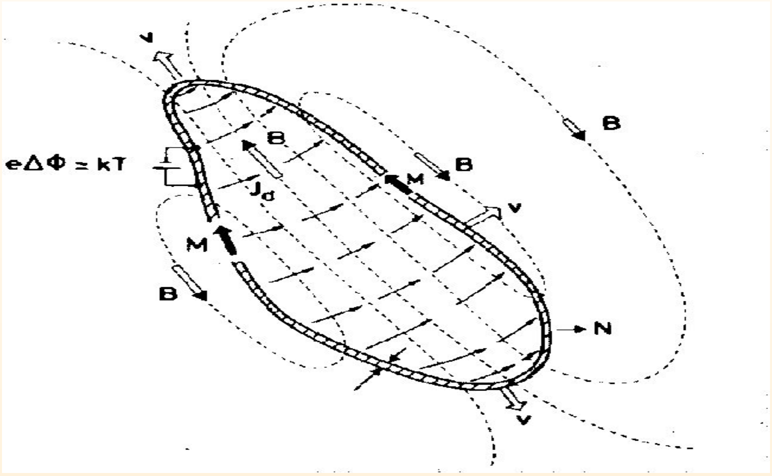

- plasma bulk velocity: $\boldsymbol{u} \approx \boldsymbol{u}^{+}$

$$\boldsymbol{u}^{\pm} = \frac{\boldsymbol{E} \times \boldsymbol{B}}{B^2} \pm \frac{m^{\pm} {V_{\perp}}^2}{2qB^3} \boldsymbol{B} \times \boldsymbol{\nabla}(B) \quad (1)$$

Collective dynamics of plasma irregularities

- plasmoids: laboratory (Bostick, 1956), active experiments in space (Haerendel, 1976), large active space structures (Hastings and Gatsonis, 1989), magnetotail (Hones, 1982), solar ejecta (Burlaga, 1982), magnetosheath (Lemaire and Roth, 1981)

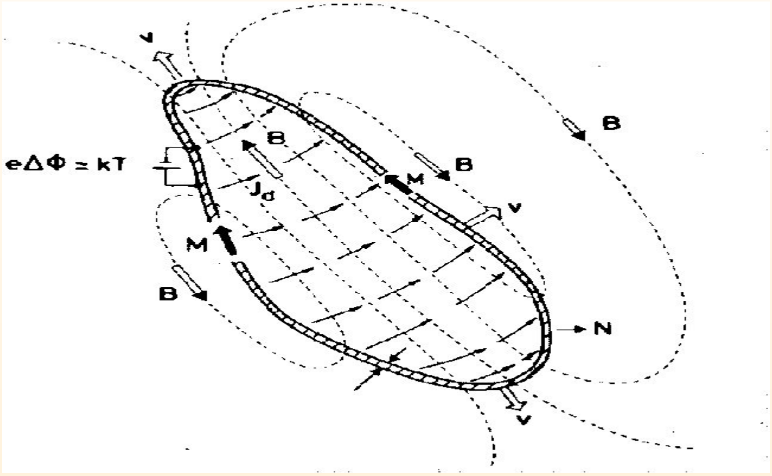

- plasma bulk velocity: $\boldsymbol{u} \approx \boldsymbol{u}^{+}$

$$\boldsymbol{u}^{\pm} = \frac{\boldsymbol{E} \times \boldsymbol{B}}{B^2} \pm \frac{m^{\pm} {V_{\perp}}^2}{2qB^3} \boldsymbol{B} \times \boldsymbol{\nabla}(B) \quad (1)$$

- plasma "slipping" (Alfvén and Fälthammar, 1963)

Collective dynamics of plasma irregularities

- plasmoids: laboratory (Bostick, 1956), active experiments in space (Haerendel, 1976), large active space structures (Hastings and Gatsonis, 1989), magnetotail (Hones, 1982), solar ejecta (Burlaga, 1982), magnetosheath (Lemaire and Roth, 1981)

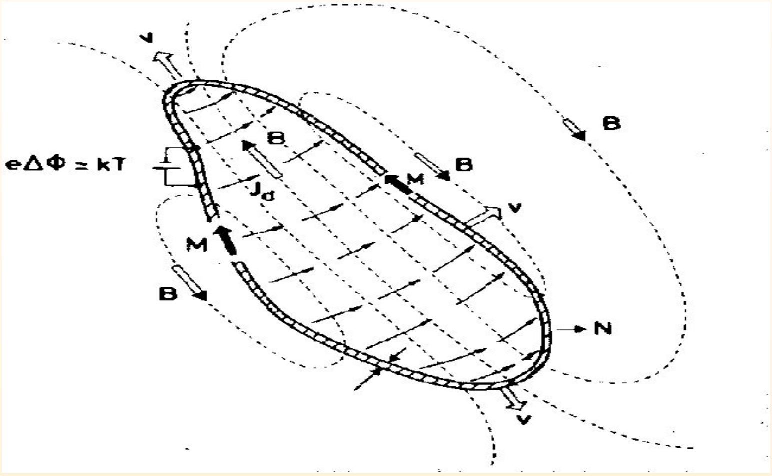

- plasma bulk velocity: $\boldsymbol{u} \approx \boldsymbol{u}^+$

$$\boldsymbol{u}^{\pm} = \frac{\boldsymbol{E} \times \boldsymbol{B}}{B^2} \pm \frac{m^{\pm} {V_{\perp}}^2}{2qB^3} \boldsymbol{B} \times \boldsymbol{\nabla}(B) \qquad (1)$$

- plasma "slipping" (Alfvén and Fälthammar, 1963)
- collective effects: diamagnetism; boundary space charge layers; field aligned potential drops/weak double layers (Lemaire and Roth, 1991)

Distribution of the electric field

- perpendicular component: polarization field due the to first order differential drifts of electrons and ions forming the plasma cloud (Schmidt, 1960; Lemaire, 1985)

$$\frac{d}{dt}\left(\frac{\boldsymbol{E}\times\boldsymbol{B}}{B^2}\right)+\frac{\overline{\mu^+}+\overline{\mu^-}}{m^+}\boldsymbol{\nabla}\left|\boldsymbol{B}\right|\cong 0 \tag{2}$$

Distribution of the electric field

- perpendicular component: polarization field due the to first order differential drifts of electrons and ions forming the plasma cloud (Schmidt, 1960; Lemaire, 1985)

$$\frac{d}{dt}\left(\frac{\boldsymbol{E}\times\boldsymbol{B}}{B^2}\right)+\frac{\overline{\mu^+}+\overline{\mu^-}}{m^+}\boldsymbol{\nabla}\left|\boldsymbol{B}\right|\cong 0 \tag{2}$$

- parallel component: weak-double layers due to the velocity shear and/or inhomogeneities of the density and temperature at the interface discontinuity (Block, 1972; Lemaire and Scherer, 1978; Raadu, 1988; Carlqvist, 1995)

Distribution of the electric field

- perpendicular component: polarization field due the to first order differential drifts of electrons and ions forming the plasma cloud (Schmidt, 1960; Lemaire, 1985)

$$\frac{d}{dt}\left(\frac{\boldsymbol{E}\times\boldsymbol{B}}{B^2}\right)+\frac{\overline{\mu^+}+\overline{\mu^-}}{m^+}\boldsymbol{\nabla}\left|\boldsymbol{B}\right|\cong 0 \qquad (2)$$

- parallel component: weak-double layers due to the velocity shear and/or inhomogeneities of the density and temperature at the interface discontinuity (Block, 1972; Lemaire and Scherer, 1978; Raadu, 1988; Carlqvist, 1995)

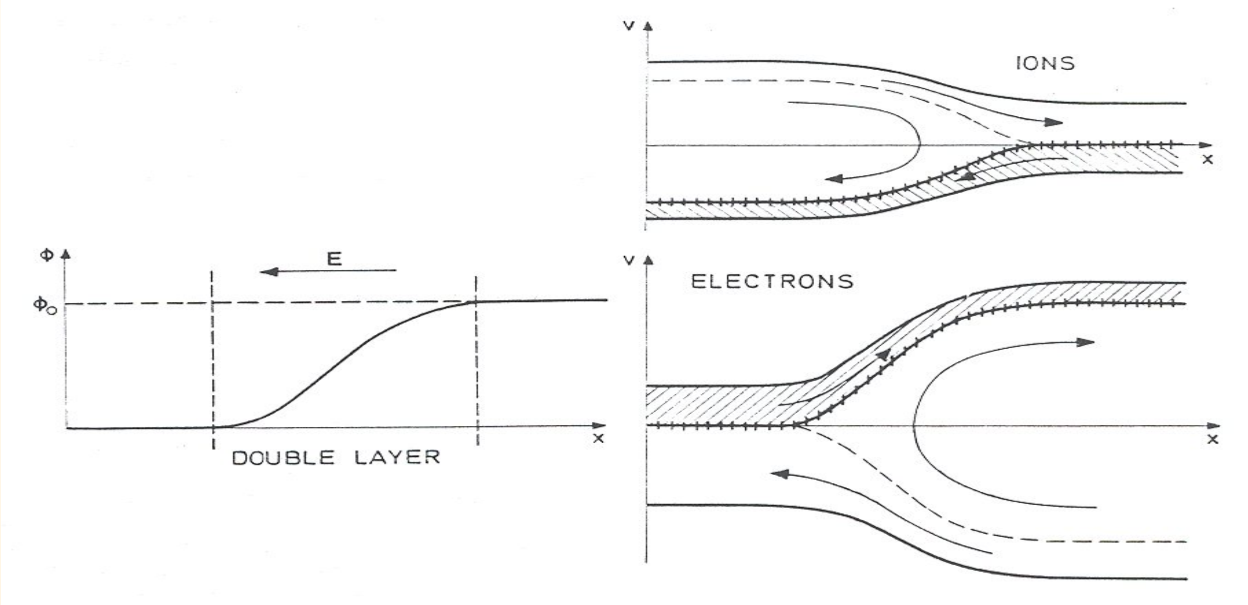

Numerical simulations - results

Infinitely long (cylindrical) filaments:

Numerical simulations - results

Infinitely long (cylindrical) filaments:

- ideal MHD: simulate penetration only for strict alignment of $\boldsymbol{B}$ in 2D geometry (Huba, 1996; Dai and Woodward, 1997);
- resistive MHD: simulate penetration for a small cone angle ($< 6^0$) in 2D geometry (Ma et al., 1991)
- hybrid: simulate penetration only for strict alignment in 2D geometry (Savoini and Scholer, 1994, 1996)

Numerical simulations - results

Infinitely long (cylindrical) filaments:

- ideal MHD: simulate penetration only for strict alignment of $\boldsymbol{B}$ in 2D geometry (Huba, 1996; Dai and Woodward, 1997);
- resistive MHD: simulate penetration for a small cone angle ($< 6^0$) in 2D geometry (Ma et al., 1991)
- hybrid: simulate penetration only for strict alignment in 2D geometry (Savoini and Scholer, 1994, 1996)

2D and 3D clouds of (macro)ions and (macro)electrons:

Numerical simulations - results

Infinitely long (cylindrical) filaments:

- ideal MHD: simulate penetration only for strict alignment of $\boldsymbol{B}$ in 2D geometry (Huba, 1996; Dai and Woodward, 1997);
- resistive MHD: simulate penetration for a small cone angle ($< 6^0$) in 2D geometry (Ma et al., 1991)
- hybrid: simulate penetration only for strict alignment in 2D geometry (Savoini and Scholer, 1994, 1996)

2D and 3D clouds of (macro)ions and (macro)electrons:

- PIC: propagation of large gyroradius(Livesey and Pritchett, 1989) and respectively small gyroradius (Neubert et al., 1992; Nishikawa, 1997) plasma clouds by polarization electric field

(a complete review in Echim and Lemaire, Space Science Reviews, 92, 565-601, 2000)

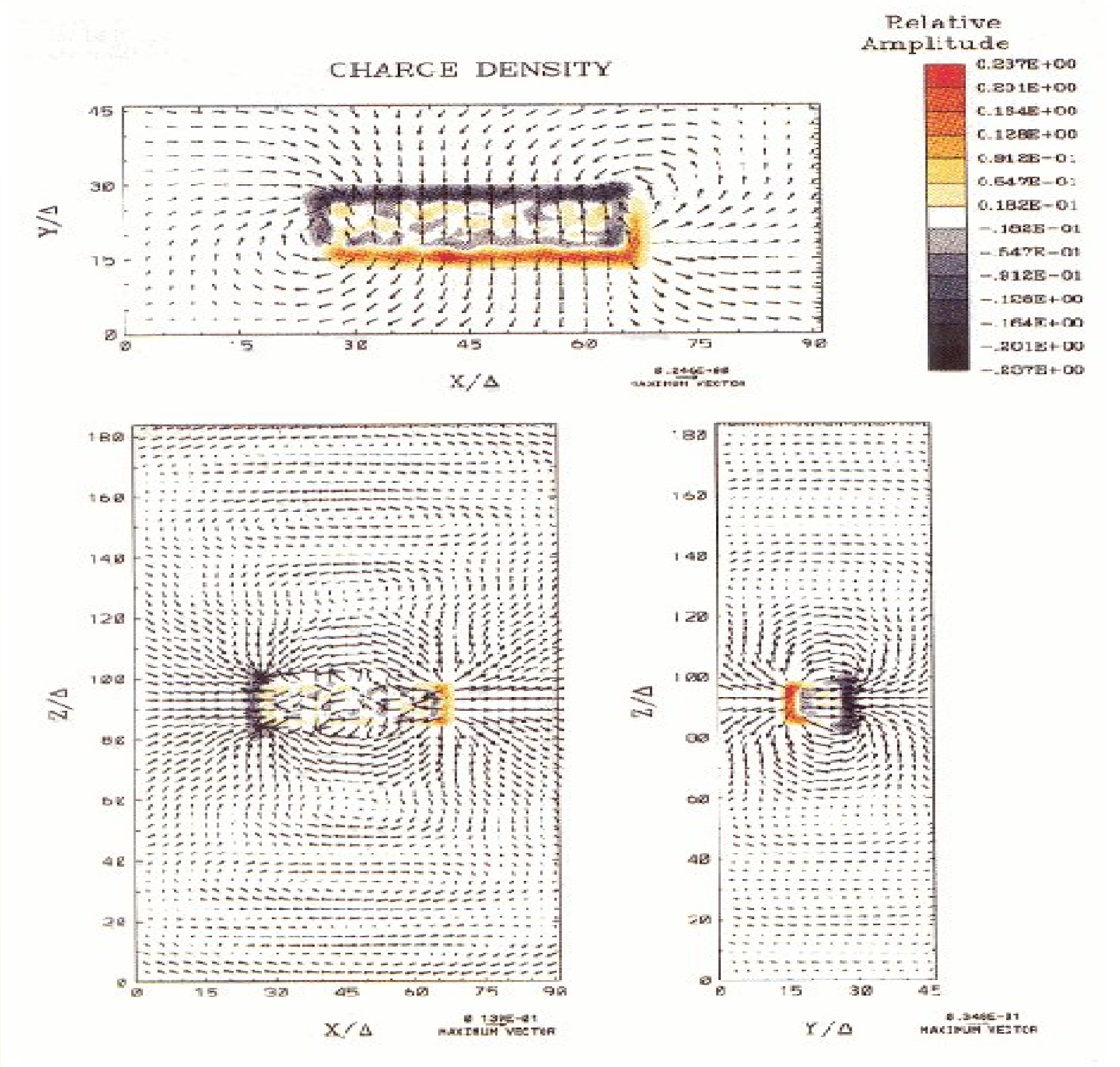

3D small gyroradius plasma cloud moving across a uniform magnetic field (Neubert et al., 1992)

Numerical integration of test-orbits

Equations:

$$\frac{d^2\boldsymbol{r}}{dt^2} = \frac{q}{m}\left[\boldsymbol{E} + \frac{d\boldsymbol{r}}{dt} \times \boldsymbol{B}\right]$$

Numerical integration of test-orbits

Equations:

$$\frac{d^2\boldsymbol{r}}{dt^2} = \frac{q}{m}\left[\boldsymbol{E} + \frac{d\boldsymbol{r}}{dt} \times \boldsymbol{B}\right]$$

$$\frac{d\boldsymbol{r}_{\boldsymbol{gc},\perp}}{dt} = \boldsymbol{v}_{gc,\perp}$$

Numerical integration of test-orbits

Equations:

$$\frac{d^2\boldsymbol{r}}{dt^2} = \frac{q}{m}\left[\boldsymbol{E} + \frac{d\boldsymbol{r}}{dt} \times \boldsymbol{B}\right]$$

$$\frac{d\boldsymbol{r}_{\boldsymbol{gc},\perp}}{dt} = \boldsymbol{v}_{gc,\perp}$$

$$\frac{d^2\boldsymbol{r}_{\boldsymbol{gc},\parallel}}{dt^2} = \frac{d\boldsymbol{v}_{gc,\parallel}}{dt}$$

Numerical integration of test-orbits

Equations:

$$\begin{aligned}
\frac{d^2\boldsymbol{r}}{dt^2} &= \frac{q}{m}\left[\boldsymbol{E} + \frac{d\boldsymbol{r}}{dt} \times \boldsymbol{B}\right] \\
\frac{d\boldsymbol{r}_{\boldsymbol{gc},\perp}}{dt} &= \boldsymbol{v}_{gc,\perp} \\
\frac{d^2\boldsymbol{r}_{\boldsymbol{gc},\parallel}}{dt^2} &= \frac{d\boldsymbol{v}_{gc,\parallel}}{dt}
\end{aligned} \qquad (3)$$

where:

$$\begin{aligned}
\boldsymbol{v}_{gc,\perp} &= \frac{\boldsymbol{E} \times \boldsymbol{B}}{B^2} + \frac{m{V_\perp}^2}{2qB^3}\boldsymbol{B} \times \boldsymbol{\nabla}(B) + \frac{m{v_\parallel}^2}{qB^4}\boldsymbol{B} \times (\boldsymbol{B} \cdot \boldsymbol{\nabla})\,\boldsymbol{B} \\
&\quad + \frac{m}{qB^2}\boldsymbol{B} \times \frac{d}{dt}\left(\frac{\boldsymbol{E} \times \boldsymbol{B}}{B^2}\right)
\end{aligned}$$

Numerical integration of test-orbits

Equations:

$$\begin{aligned} \frac{d^2\boldsymbol{r}}{dt^2} &= \frac{q}{m}\left[\boldsymbol{E} + \frac{d\boldsymbol{r}}{dt} \times \boldsymbol{B}\right] \\ \frac{d\boldsymbol{r}_{\boldsymbol{gc},\perp}}{dt} &= \boldsymbol{v}_{gc,\perp} \\ \frac{d^2\boldsymbol{r}_{\boldsymbol{gc},\parallel}}{dt^2} &= \frac{d\boldsymbol{v}_{gc,\parallel}}{dt} \end{aligned} \qquad (3)$$

where:

$$\begin{aligned} \boldsymbol{v}_{gc,\perp} &= \frac{\boldsymbol{E} \times \boldsymbol{B}}{B^2} + \frac{m{V_\perp}^2}{2qB^3}\boldsymbol{B} \times \boldsymbol{\nabla}(B) + \frac{m{v_\parallel}^2}{qB^4}\boldsymbol{B} \times (\boldsymbol{B} \cdot \boldsymbol{\nabla})\,\boldsymbol{B} \\ &\quad + \frac{m}{qB^2}\boldsymbol{B} \times \frac{d}{dt}\left(\frac{\boldsymbol{E} \times \boldsymbol{B}}{B^2}\right) \\ \frac{dv_{gc,\parallel}}{dt} &= \boldsymbol{U}_E \cdot \left(\frac{\partial \boldsymbol{b}}{\partial t} + v_{gc,\parallel}\frac{\partial \boldsymbol{b}}{\partial s} + \boldsymbol{U}_E \cdot \boldsymbol{\nabla}\boldsymbol{b}\right) \frac{q}{m}E_\parallel - \frac{\mu}{m}\frac{\partial B}{\partial s} \end{aligned}$$

Numerical integration of test-orbits

Equations:

$$\begin{aligned}
\frac{d^2\boldsymbol{r}}{dt^2} &= \frac{q}{m}\left[\boldsymbol{E} + \frac{d\boldsymbol{r}}{dt} \times \boldsymbol{B}\right] \\
\frac{d\boldsymbol{r_{gc,\perp}}}{dt} &= \boldsymbol{v}_{gc,\perp} \\
\frac{d^2\boldsymbol{r_{gc,\parallel}}}{dt^2} &= \frac{d\boldsymbol{v}_{gc,\parallel}}{dt}
\end{aligned} \tag{3}$$

where:

$$\begin{aligned}
\boldsymbol{v}_{gc,\perp} &= \frac{\boldsymbol{E}\times\boldsymbol{B}}{B^2} + \frac{m{V_\perp}^2}{2qB^3}\boldsymbol{B}\times\boldsymbol{\nabla}(B) + \frac{m{v_\parallel}^2}{qB^4}\boldsymbol{B}\times(\boldsymbol{B}\cdot\boldsymbol{\nabla})\,\boldsymbol{B} \\
&\quad + \frac{m}{qB^2}\boldsymbol{B}\times\frac{d}{dt}\left(\frac{\boldsymbol{E}\times\boldsymbol{B}}{B^2}\right) \\
\frac{dv_{gc,\parallel}}{dt} &= \boldsymbol{U}_E\cdot\left(\frac{\partial\boldsymbol{b}}{\partial t} + v_{gc,\parallel}\frac{\partial\boldsymbol{b}}{\partial s} + \boldsymbol{U}_E\cdot\boldsymbol{\nabla}\boldsymbol{b}\right)\frac{q}{m}E_\parallel - \frac{\mu}{m}\frac{\partial B}{\partial s}
\end{aligned}$$

Electromagnetic field for integration

Electric field

- CASE A: uniform electric field

  $$\boldsymbol{E}(x) = \boldsymbol{E}_A = cst = -\boldsymbol{v}_{gc_1} \times \boldsymbol{B}_1$$

Electromagnetic field for integration

Electric field

- CASE A: uniform electric field

$$\boldsymbol{E}(x) = \boldsymbol{E}_A = cst = -\boldsymbol{v}_{gc_1} \times \boldsymbol{B}_1 \tag{4}$$

- CASE B: non-uniform, conserving U_E

$$\boldsymbol{E}_B(x) = -\boldsymbol{v}_{gc_1} \times \boldsymbol{B}(x)$$

Electromagnetic field for integration

Electric field

- CASE A: uniform electric field

$$\boldsymbol{E}(x) = \boldsymbol{E}_A = cst = -\boldsymbol{v}_{gc_1} \times \boldsymbol{B}_1 \tag{4}$$

- CASE B: non-uniform, conserving U_E

$$\boldsymbol{E}_B(x) = -\boldsymbol{v}_{gc_1} \times \boldsymbol{B}(x) \tag{5}$$

- CASE C: non-uniform, conserving $\overline{\mu^+} + \overline{\mu^-}$

$$\frac{d}{dt}\left(\frac{\boldsymbol{E}_c(x) \times \boldsymbol{B}(x)}{B^2}\right) + \frac{\overline{\mu^+} + \overline{\mu^-}}{m^+}\boldsymbol{\nabla}\left|\boldsymbol{B}(x)\right| \cong 0$$

Electromagnetic field for integration

Electric field

- CASE A: uniform electric field

$$\boldsymbol{E}(x) = \boldsymbol{E}_A = cst = -\boldsymbol{v}_{gc_1} \times \boldsymbol{B}_1 \tag{4}$$

- CASE B: non-uniform, conserving U_E

$$\boldsymbol{E}_B(x) = -\boldsymbol{v}_{gc_1} \times \boldsymbol{B}(x) \tag{5}$$

- CASE C: non-uniform, conserving $\overline{\mu^+} + \overline{\mu^-}$

$$\frac{d}{dt}\left(\frac{\boldsymbol{E}_c(x) \times \boldsymbol{B}(x)}{B^2}\right) + \frac{\overline{\mu^+} + \overline{\mu^-}}{m^+}\boldsymbol{\nabla}\left|\boldsymbol{B}(x)\right| \cong 0 \tag{6}$$

Magnetic field : tangential discontinuity

$$\boldsymbol{B}(x) = \frac{\boldsymbol{B}_1}{2} erfc\left(\frac{x}{L}\right) + \frac{\boldsymbol{B}_2}{2}\left[2 - erfc\left(\frac{x}{L}\right)\right]$$

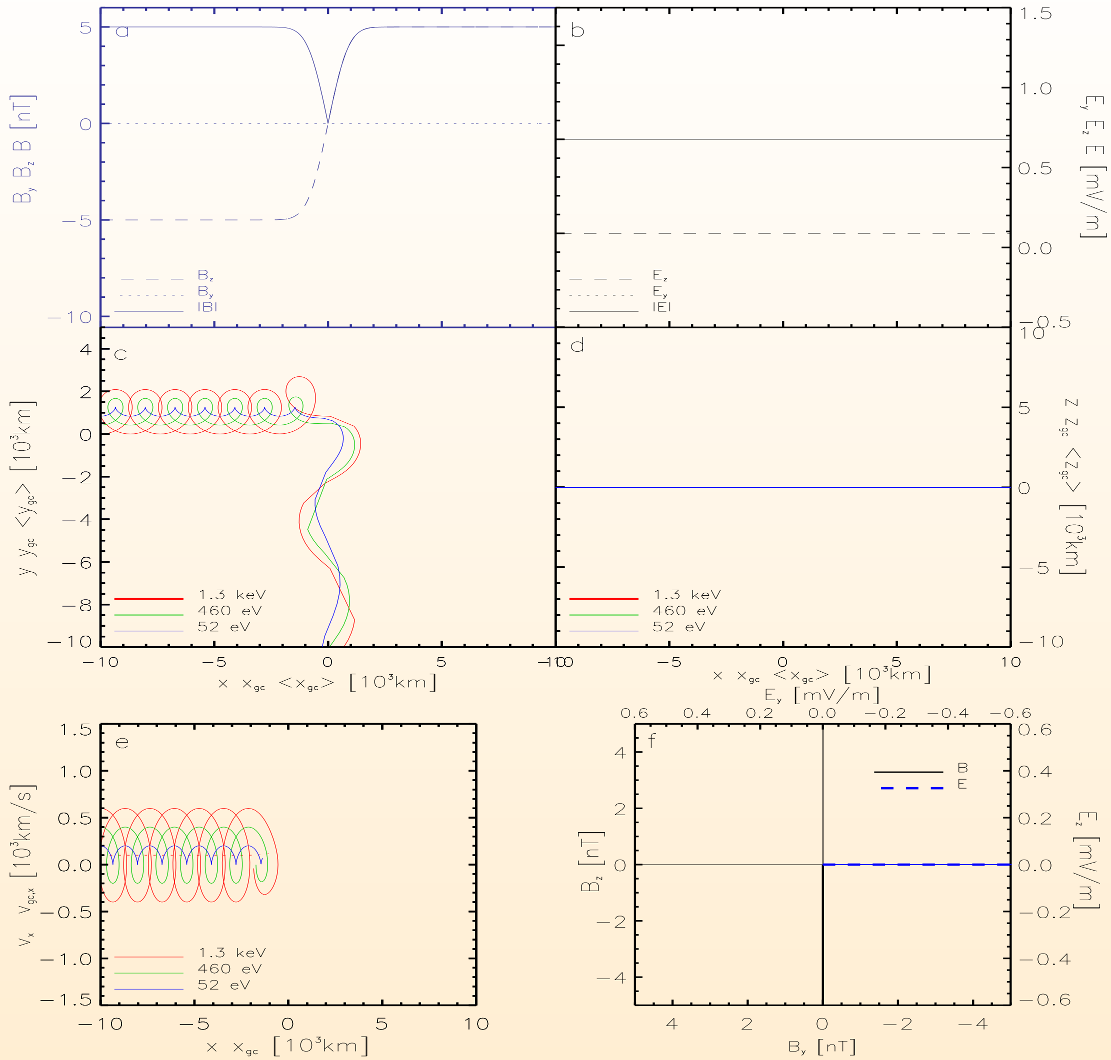

electric field distribution of CASE A

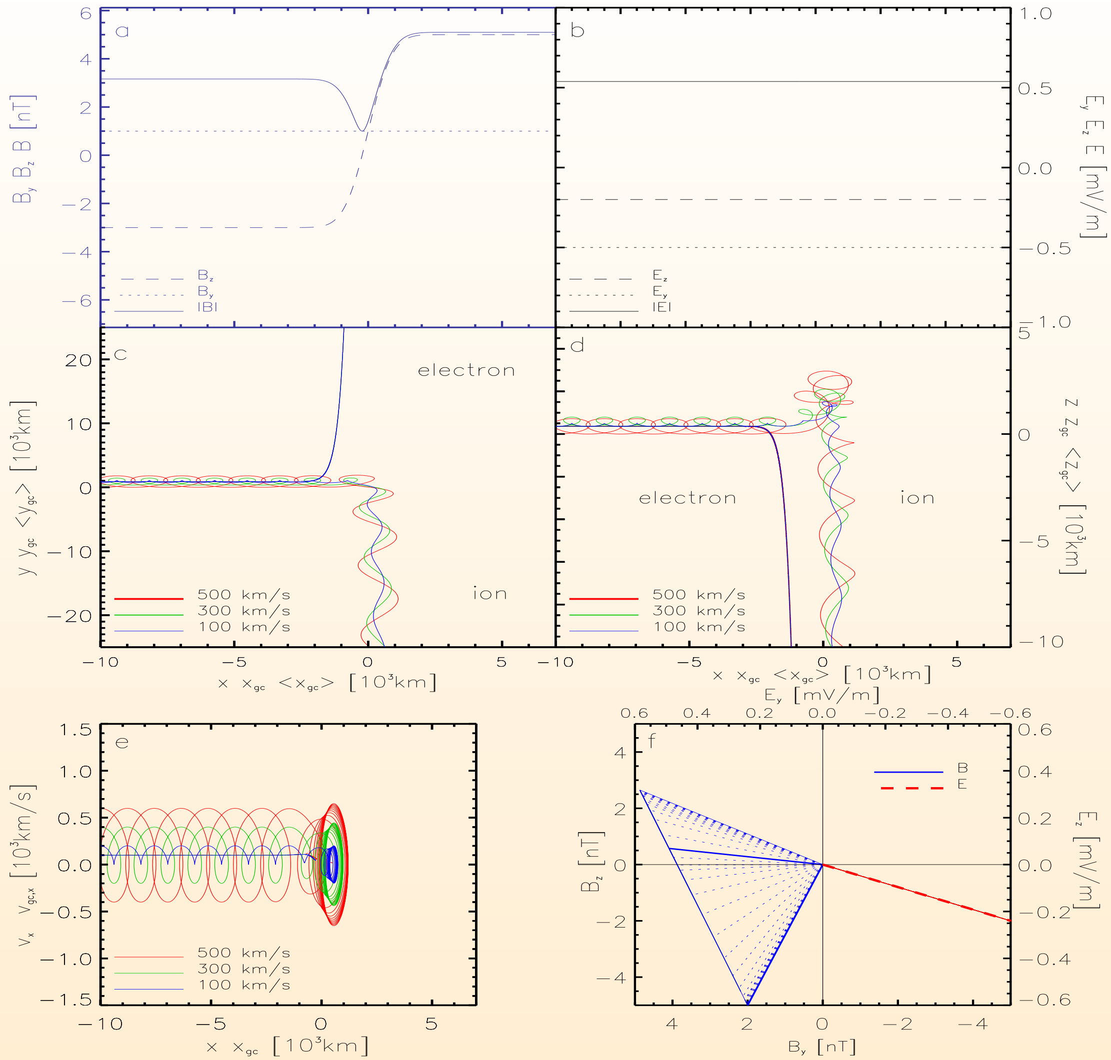

electric field distribution of CASE A

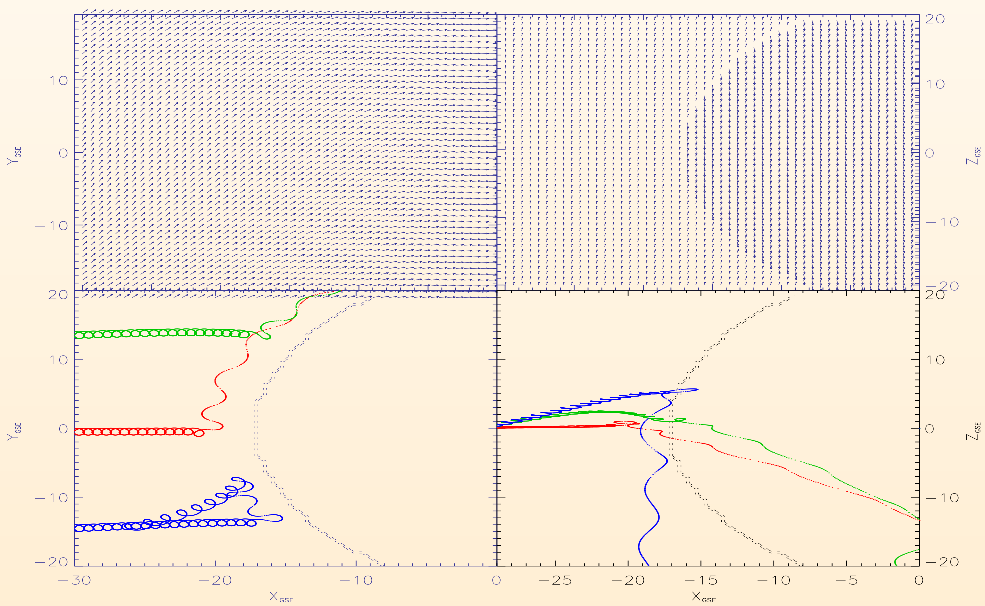

3D electric field distribution of CASE A with magnetopause model from Shue et al. (1997)

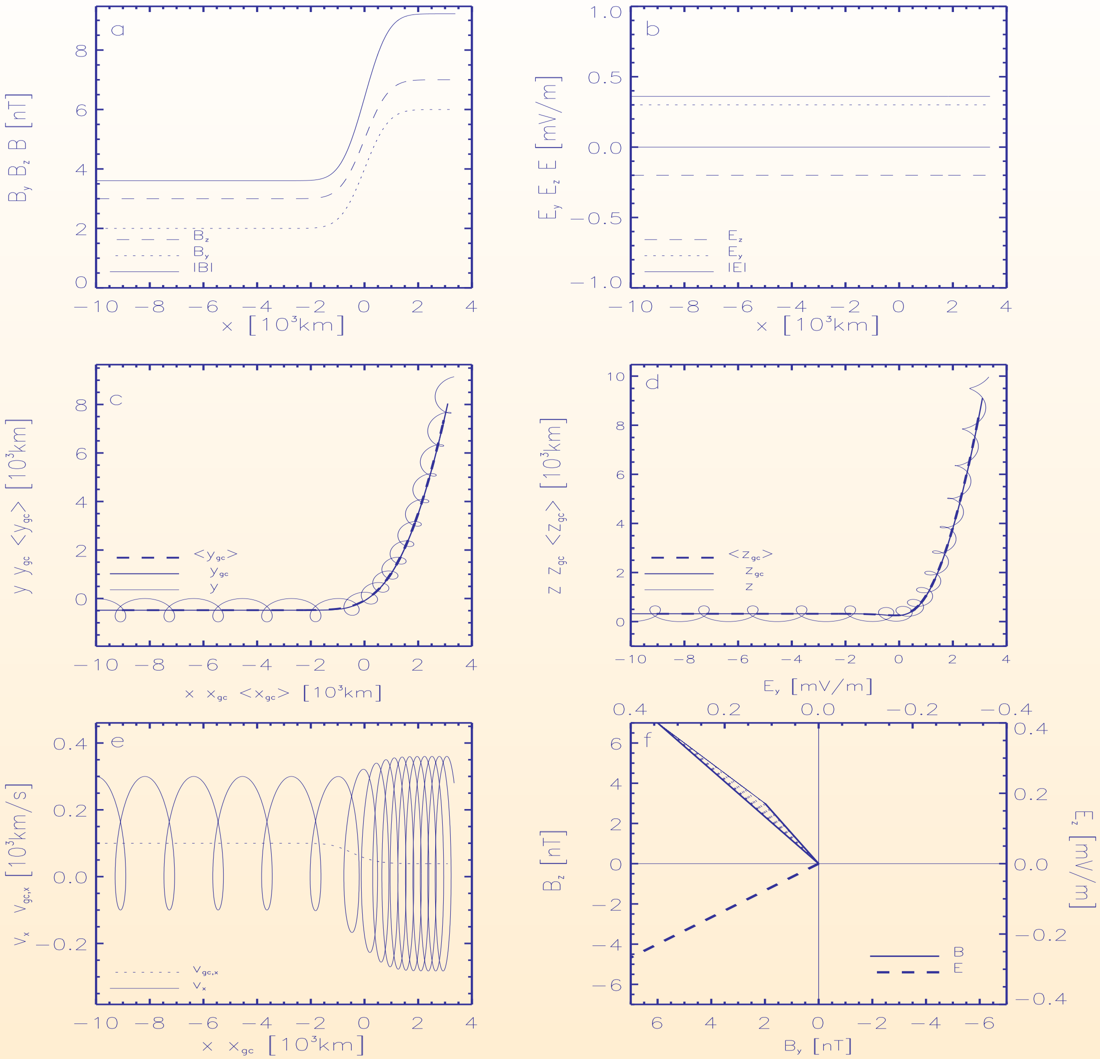

electric field distribution of CASE A

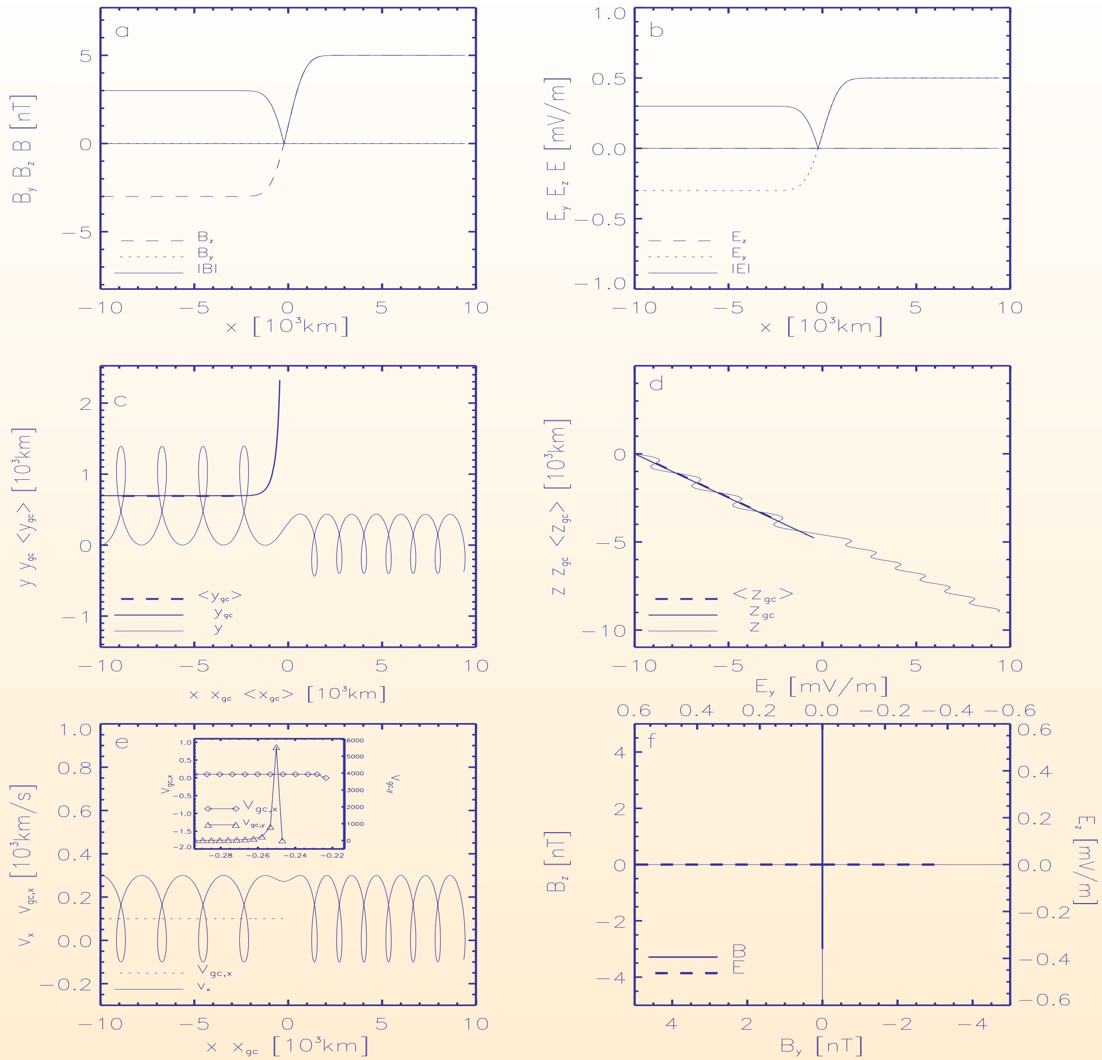

electric field distribution of CASE B

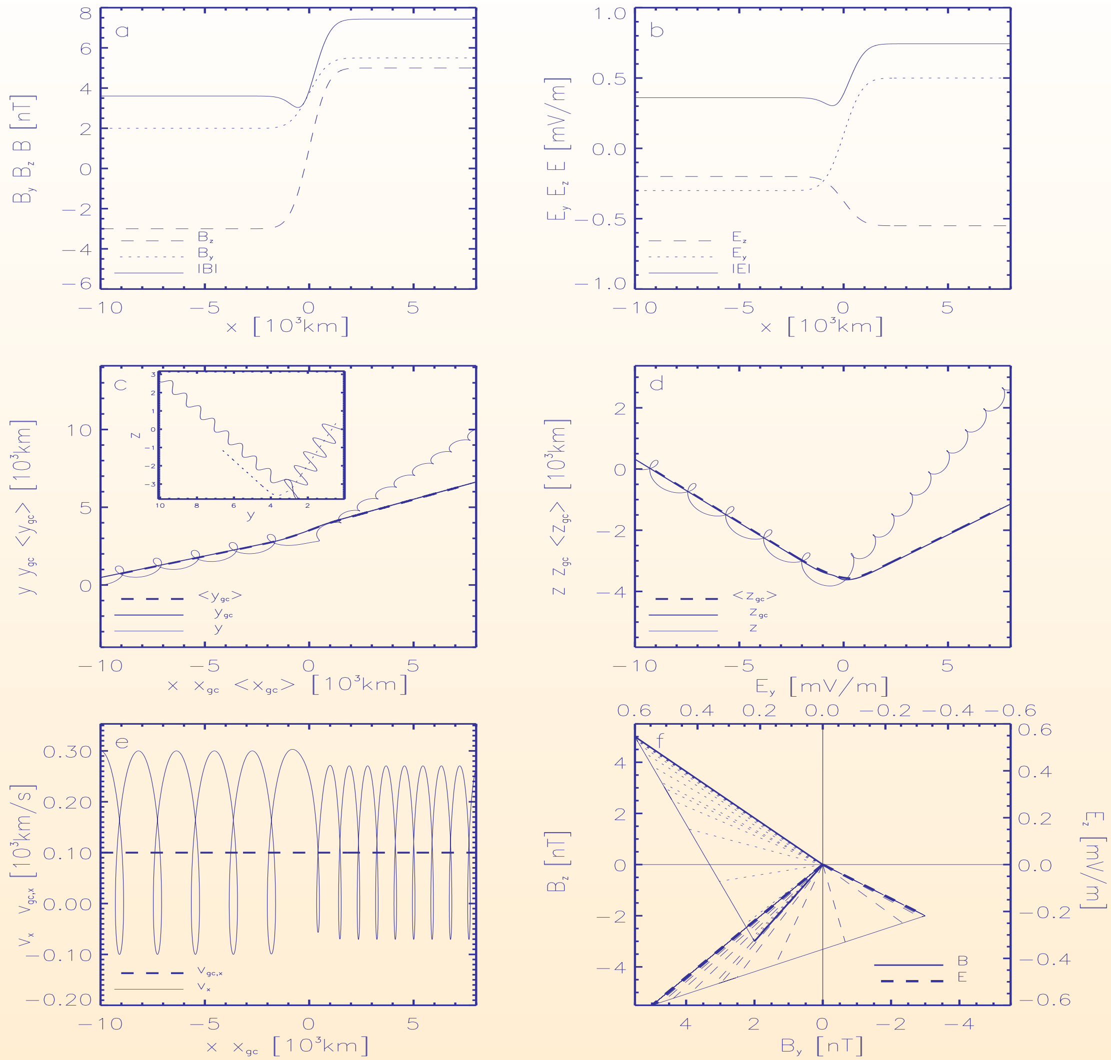

electric field distribution of CASE B

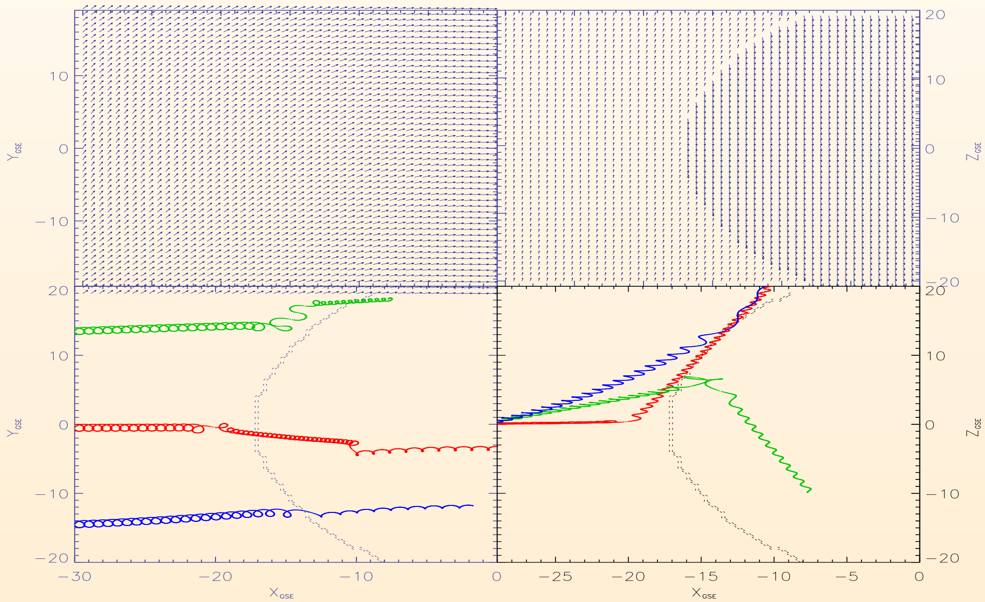

3D electric field distribution of CASE B with magnetopause model from Shue et al. (1997)

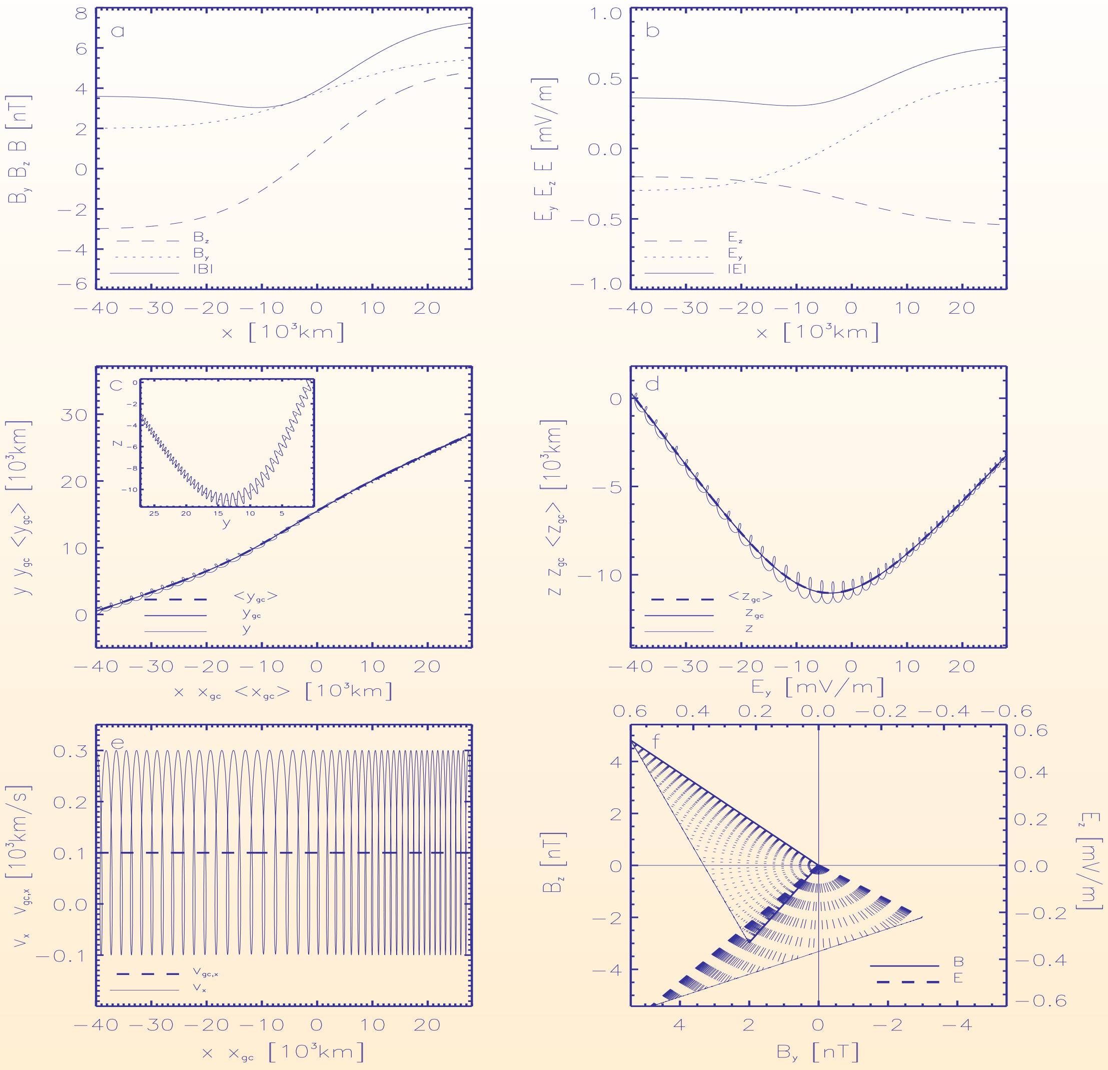

electric field distribution of CASE B

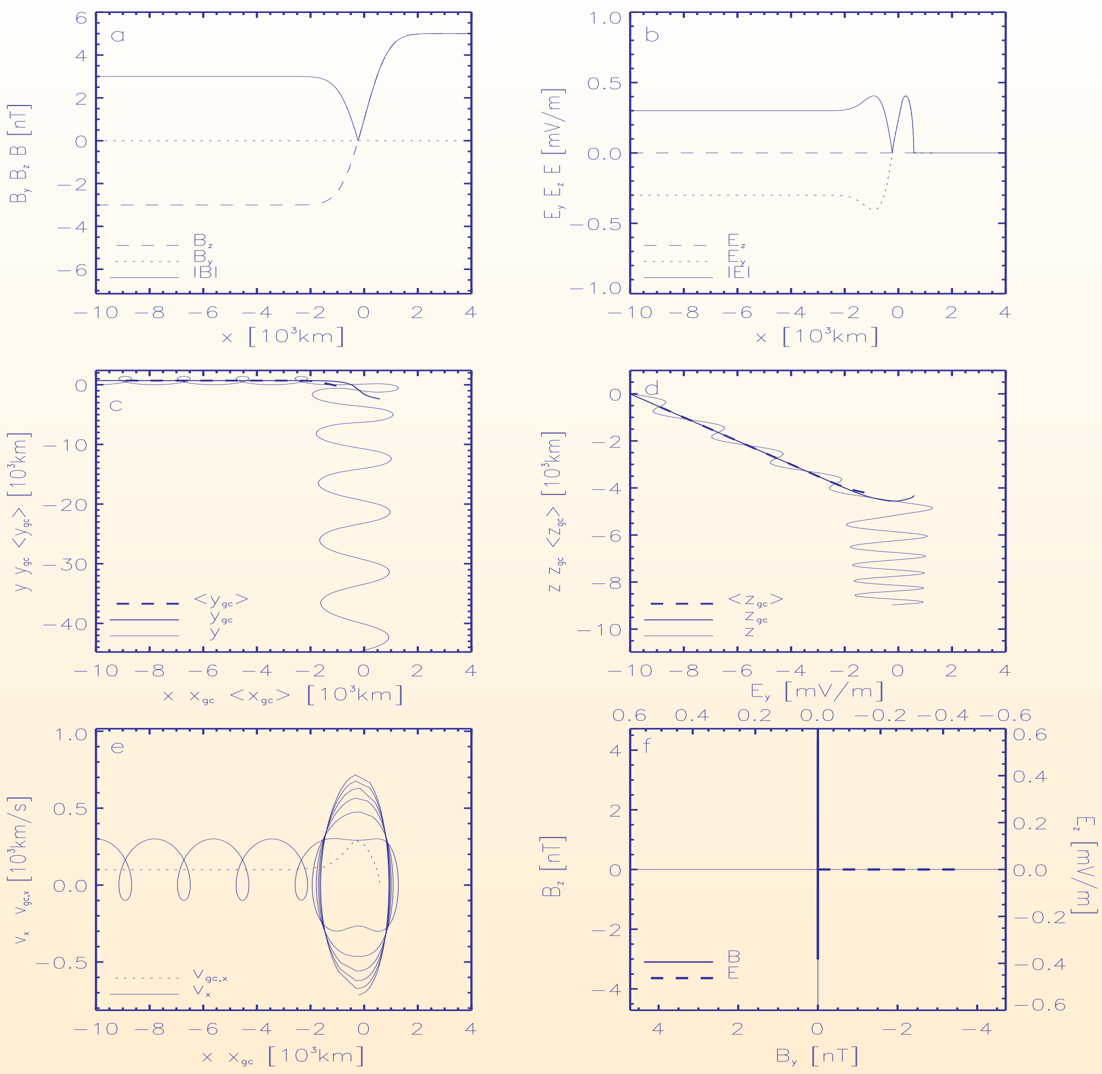

electric field distribution of CASE C

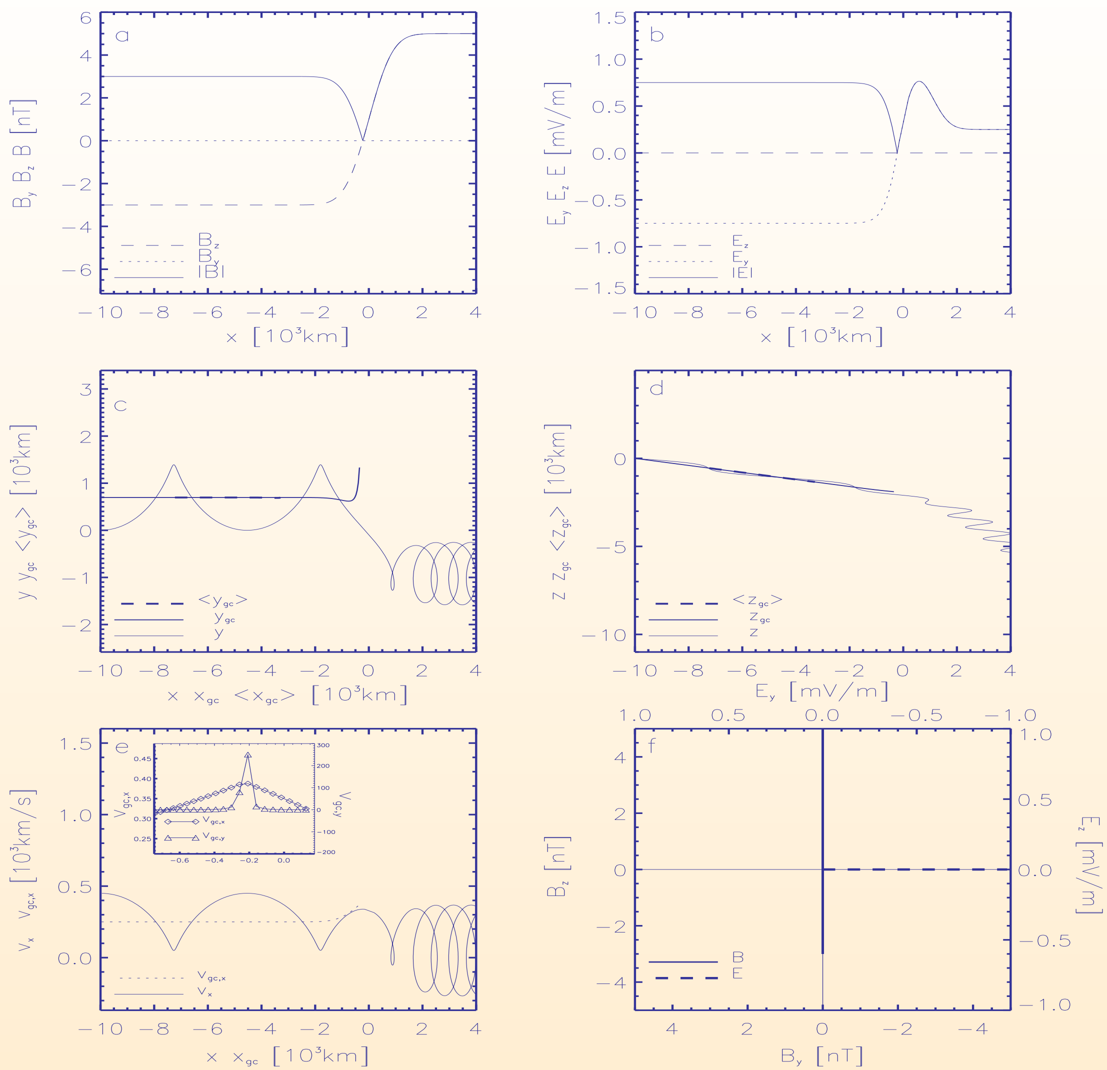

electric field distribution of CASE C

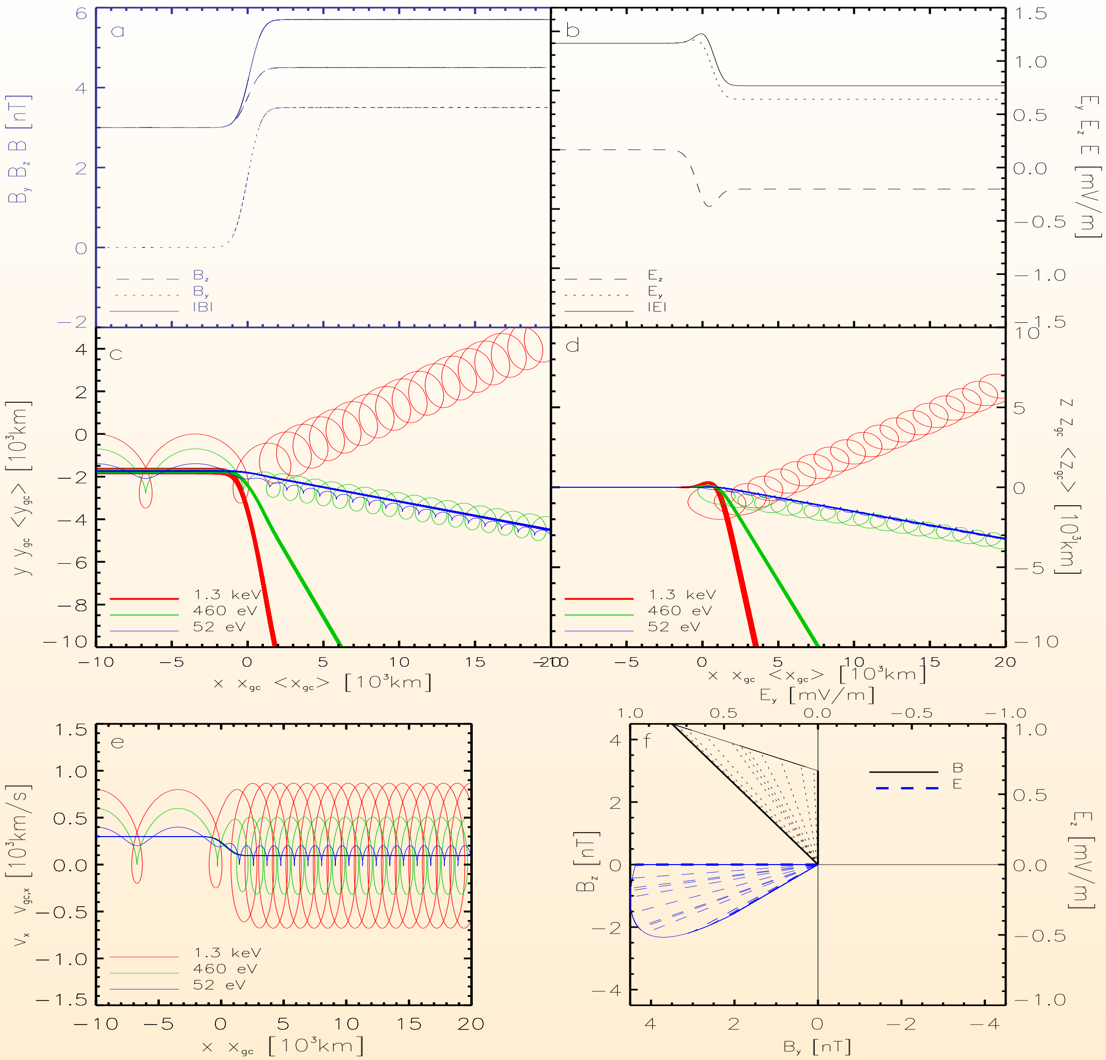

electric field distribution of CASE C

Conclusions

- three dimensional (localized) plasma structures propagate across magnetic field; the motion is sustained by a self-polarization electric field due to space charge layers at the structure edges.

Conclusions

- three dimensional (localized) plasma structures propagate across magnetic field; the motion is sustained by a self-polarization electric field due to space charge layers at the structure edges.
- single particle trajectories deflect along a TD magnetopause in the case of a uniform E-field distribution; the zero and guiding center approximations diverge; a non-classical process (magnetic reconnection) is required to enable plasma transfer across the magnetopause (Mozer et al., 2002). The exact equation of motion HAS NO SINGULAR POINTS.

Conclusions

- three dimensional (localized) plasma structures propagate across magnetic field; the motion is sustained by a self-polarization electric field due to space charge layers at the structure edges.
- single particle trajectories deflect along a TD magnetopause in the case of a uniform E-field distribution; the zero and guiding center approximations diverge; a non-classical process (magnetic reconnection) is required to enable plasma transfer across the magnetopause (Mozer et al., 2002). The exact equation of motion HAS NO SINGULAR POINTS.
- other, non-uniform E-field distribution can be imagined (cases B and C above), enabling single particle trajectories to penetrate the magnetopause. Non-classical processes are not required for mass transfer across B-field lines.

Conclusions

- three dimensional (localized) plasma structures propagate across magnetic field; the motion is sustained by a self-polarization electric field due to space charge layers at the structure edges.
- single particle trajectories deflect along a TD magnetopause in the case of a uniform E-field distribution; the zero and guiding center approximations diverge; a non-classical process (magnetic reconnection) is required to enable plasma transfer across the magnetopause (Mozer et al., 2002). The exact equation of motion HAS NO SINGULAR POINTS.
- other, non-uniform E-field distribution can be imagined (cases B and C above), enabling single particle trajectories to penetrate the magnetopause. Non-classical processes are not required for mass transfer across B-field lines.

- ▷ *Models for plasma*
- ▷ *Collective dynamics*
- ▷ *E-field distribution*
- ▷ *Global numerical simulations*
- ▷ *Sample PIC*
- ▷ *Equations to integrate*
- ▷ *A1*
- ▷ *A2*
- ▷ *A3*
- ▷ *A4*
- ▷ *A5*
- ▷ *A6*
- ▷ *A7*
- ▷ *A8*
- ▷ *A9*
- ▷ *A10*
- ▷ *A11*
- ▷ *Conclusions*